

Polymer Chemistry

Accepted Manuscript



This is an *Accepted Manuscript*, which has been through the Royal Society of Chemistry peer review process and has been accepted for publication.

Accepted Manuscripts are published online shortly after acceptance, before technical editing, formatting and proof reading. Using this free service, authors can make their results available to the community, in citable form, before we publish the edited article. We will replace this *Accepted Manuscript* with the edited and formatted *Advance Article* as soon as it is available.

You can find more information about *Accepted Manuscripts* in the [Information for Authors](#).

Please note that technical editing may introduce minor changes to the text and/or graphics, which may alter content. The journal's standard [Terms & Conditions](#) and the [Ethical guidelines](#) still apply. In no event shall the Royal Society of Chemistry be held responsible for any errors or omissions in this *Accepted Manuscript* or any consequences arising from the use of any information it contains.

Conjugated Microporous Copolymer Networks with Enhanced Gas Adsorption

Miao Yu, Xiaoyan Wang, Xiao Yang, Yang Zhao, Jia-Xing Jiang*

School of Materials Science and Engineering, Shaanxi Normal University, Xi'an, 710062, Shaanxi, P. R. China

E-mail: jiaxing@smu.edu.cn

Abstract

A series of copolymerized conjugated microporous polymers (CP-CMPs) has been synthesized by Suzuki cross-coupling copolymerization of 1,4-benzene diboronic acid with comonomers of 1,3,6,8-tetrabromopyrene and/or 1,3,6,8-tetrabromocarbazole at different ratios. These CP-CMPs are stable in common organic solvents and thermally stable. It was found that the ratio of comonomers has a large influence on the pore properties of these CP-CMPs such as apparent Brunauer-Emmet-Teller (BET) specific surface area, micropore surface area and micropore volume. CP-CMP5 with 60 mol% 1,3,6,8-tetrabromocarbazole shows a high BET specific surface area up to 2241 m² g⁻¹ and a high CO₂ uptake ability of 4.57 mmol g⁻¹ (1.13 bar/273 K) with a H₂ uptake ability of 2.24 wt% (1.13 bar/77.3 K). These results demonstrate that copolymerization is an efficient strategy to tune the pore properties of microporous organic polymers, and would be promising for producing other type microporous organic polymers with high level of porosity and CO₂ uptake ability.

Keywords: conjugated microporous polymer, copolymerization, carbazole, gas adsorption.

Introduction

The excessive emission of CO₂ produced from the burning of fossil fuels has led to global climate change and some environment issues. Therefore, it is highly desirable to develop viable carbon capture and separation technologies (CCS) for capturing efficiently CO₂ and preventing environmental degradation. The current leading CO₂ capture technology is amine-based wet scrubbing technology,¹ however, this process needs relatively high energy penalty to regenerate the amine solution after CO₂ capture, which leads to the high cost. Recent studies have revealed that porous solid adsorbents, such as zeolites,² activated carbons,³ metal-organic frameworks (MOFs),⁴ and porous organic polymers (POPs),⁵ to be promising for capturing CO₂, which physisorb CO₂ molecules via weak van der Waals forces making the regeneration of the materials energy much more efficient. Among these porous solid materials, POPs have attracted significant recent interest due to their high surface area, tunable pore properties, excellent physicochemical stability, and synthetic diversification, which make them strong candidates for CO₂ capture and separation. In the past decade, a variety of POPs including polymers of intrinsic microporosity (PIMs),⁶ hypercrosslinked porous polymers (HCPs),⁷ covalent organic frameworks (COFs),⁸ conjugated microporous polymers (CMPs),⁹ and porous aromatic frameworks (PAFs)¹⁰ have been proposed for capture of CO₂.

As a sub-class of POPs, CMPs^{11, 12} that combine π -conjugation structure with high surface area and permanent nanopores have been intensively explored as gas adsorbents,¹³ supercapacitors,¹⁴ light-harvesting materials,¹⁵ light-emitting materials,^{16,} ¹⁷ optoelectronic materials¹⁸ and photocatalysts.¹⁹⁻²² In the past years, most efforts have been focused on the development of novel functionalized CMPs via various building blocks and synthetic strategies for improving the gas storage performance.

For example, CMPs with chemical functionalities of carboxylic acids, amines, hydroxyl groups, or methyl groups showed high isosteric heat of sorption for CO₂,¹³ cobalt/aluminium-coordinated CMPs exhibited outstanding CO₂ capture up to 1.80 mmol g⁻¹ at 1.0 bar and 298 K,²³ CMPs from post-synthetic amine functionalization exhibited a high CO₂/N₂ adsorption selectivity of 155 at 1 bar and 298 K,²⁴ CMP impregnated with polyethylenimine showed a high CO₂ uptake ability of 2.66 mmol g⁻¹ at 0.15 atm of CO₂ pressure and 298 K.²⁵

It is well known that the surface area and pore size have large influence on the gas adsorption performance of POPs, and it has been proved that statistical copolymerization is an efficient approach to tune the pore properties of POPs. For example, the pore size of CMPs could be fine-tuned in a continuous manner via statistical copolymerization by comonomer struts with different lengths.²⁶ The CO₂/N₂ adsorption selectivity could be improved by increasing aniline content in HCPs via statistical copolymerization.²⁷ The surface area and micropore volume of HCPs could be controlled by adjusting the comonomer content of tetraphenylethylene.²⁸ The CO₂ sorption performance could be enhanced by statistical copolymerization via Yamamoto Ullmann cross-coupling reaction from tetrakis(4-bromophenyl)methane and tris(4-bromophenyl)amine.²⁹ These results demonstrated that it is possible to use a statistical mixture of comonomers in POP systems to vary properties systematically, something that is much more difficult to do in the case of crystalline porous materials such as metal-organic frameworks (MOFs), where specific stoichiometric compositions are favoured.³⁰ However, the surface area of the reported copolymer networks lies “between” both of homocoupling polymers without a second comonomer.

Here, we synthesized a series of conjugated microporous copolymer networks by

statistical copolymerization via Pd-catalyzed Suzuki coupling reaction of 1,4-benzene diboronic acid with comonomers of 1,3,6,8-tetrabromopyrene and/or 1,3,6,8-tetrabromocarbazole in a number of ratios. The resulting copolymer networks show high levels of porosity (surface areas up to $2241 \text{ m}^2 \text{ g}^{-1}$) with a high CO_2 uptake ability of 4.57 mmol g^{-1} at 1.13 bar/273 K.

Experimental section

Chemicals: Carbazole and pyrene were purchased from TCI, 1,4-benzene diboronic acid (BDA) and other chemicals were purchased from J&K Scientific Ltd. All chemicals were used as received. 1,3,6,8-tetrabromopyrene (TBrPy)³¹ and 1,3,6,8-tetrabromocarbazole (TBrCz)³² were prepared according to the previously reported methods.

Synthesis of the copolymer networks

All of the copolymer networks were synthesized by palladium(0)-catalyzed Suzuki cross-coupling polycondensation of 1,4-benzene diboronic acid with 1,3,6,8-tetrabromopyrene and/or 1,3,6,8-tetrabromocarbazole. All polymerizations were carried out at a fixed total molar monomer concentration (150 mmol/L) and a fixed reaction temperature and reaction time (150 °C/48 h). A representative experimental procedure for CP-CMP1 is given as an example.

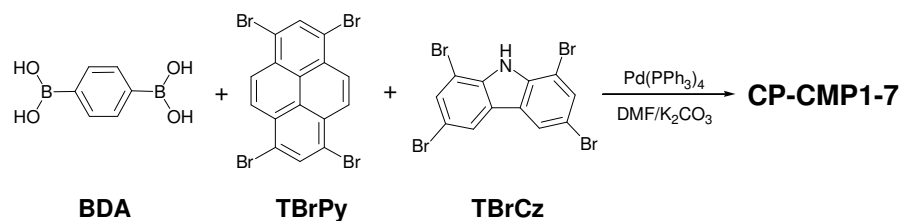
CP-CMP1: To a mixture of BDA (332 mg, 2.0 mmol) and TBrPy (518 mg, 1.0 mmol) in dimethylformamide (DMF, 20 mL), an aqueous solution of K_2CO_3 (2.0 M, 3 mL) and tetrakis(triphenylphosphine)palladium (0) (25 mg, $21.6 \mu\text{mol}$) were added. The mixture was degassed and purged with N_2 , and stirred at 150 °C for 48 h. The mixture was then cooled down to room temperature and poured into methanol. The precipitate was collected by filtration, and washed with H_2O , CHCl_3 , THF and acetone, respectively. Further purification of the polymer was carried out by Soxhlet extraction

with THF for 24 h. The product was dried in vacuum for 24 h at 70 °C as a fine green solid powder (Yield: 310 mg, 88.1%). Elemental combustion analysis (%) Calcd for C₂₈H₁₄ (based on the theoretical formula for an infinite CP-CMP1 network without any unreacted end group): C 95.97, H 4.03; Found: C 89.57, H 4.36. The deviation of the elemental analysis from that expected could be attributed to the unreacted end groups and water trapped in the sample, which was not effectively removed by the outside analysis laboratory.^{33, 34} The repeated experiment was carried out by using the same reaction conditions.

Characterization: Elemental analysis was carried out on a EURO EA3000 Elemental Analyzer. The Fourier transform infrared (FT-IR) spectra were collected in transmission on a Tensor 27 FT-IR spectrometer (Bruker) using KBr disk. The thermal properties of the copolymer networks were evaluated using a thermogravimetric analysis (TGA) – differential thermal analysis instrument (Q1000DSC+LNCS+FACS Q600SDT) over the temperature range from 30 to 800 °C under a nitrogen atmosphere with a heating rate of 10 °C/min. Surface areas and pore size distributions of the copolymer networks were measured by nitrogen adsorption and desorption at 77.3 K using an ASAP 2420-4 (Micromeritics) volumetric adsorption analyzer. The surface areas were calculated in the relative pressure range (P/P_0) from 0.05 to 0.20 using BET method. Pore size distributions and pore volumes were derived from the adsorption branches of the isotherms using the non-local density functional theory. Samples were degassed at 120 °C for 15 h under vacuum (10^{-5} bar) before analysis. Hydrogen adsorption isotherms were measured on the ASAP 2420-4 at 77.3 K up to 1.13 bar. Carbon dioxide adsorption isotherms were also collected on the ASAP 2420-4 at 273 K, and 298 K, respectively.

Results and discussion

Scheme 1 shows the general synthetic routes for the series of copolymer networks. We selected here TByPy and TBrCz as the comonomers since tetra-functionalized building blocks can afford porous polymers with high porosity and high CO₂ adsorption capacity.^{16, 35, 36} To insight into the feed ratio of the comonomers on the pore properties of the resulting copolymer networks, we prepared a series of conjugated microporous copolymers in a number of ratios. During polymerization, all of the copolymer networks precipitated from solution as green or yellow powders that were totally insoluble in common organic solvents tested because of their highly crosslinked and rigid structures. Thermogravimetric analysis indicated that all of the copolymer networks were thermally stable up to 400 °C in nitrogen atmosphere (Fig. S1). The FT-IR spectra of the copolymer networks (Fig. S2) were consistent with the expected network structure showing aromatic C=C vibration bands at 1620 cm⁻¹, the stretching vibration of the C-N-C at 1500 cm⁻¹, the N-H stretching vibration at around 3450 cm⁻¹ and the bending vibration at 1390 cm⁻¹ for CP-CMP2–7, which were not observed in the FT-IR spectrum for CP-CMP1 without carbazole unit. We need to point out that the broad peak at around 3400 cm⁻¹ in the FT-IR spectrum for CP-CMP1 might be from the physisorbed water within the networks because of its high microporosity.²⁷ The copolymer networks are amorphous in nature without showing any clear peaks in powder X-ray diffraction measurements (Fig. S3), as observed for most other reported CMP networks.^{11, 15, 16, 26} Scanning electron microscope images showed that the resulting copolymer networks consist of relatively uniform solid nano-particles (Fig. S4).



Scheme 1 Synthetic route for the copolymer networks.

The porous properties of the copolymer networks were investigated by nitrogen adsorption analyses at 77.3 K. As shown in Fig. 1a, all of the resulting copolymer networks gave rise to Type I nitrogen gas sorption isotherms with a steep nitrogen gas uptake at low relative pressure ($P/P_0 < 0.001$) indicative of micropores.³⁷ The small rise in the N_2 uptake at high relative pressures ($P/P_0 > 0.9$) in the adsorption isotherms of the copolymer networks may stem from interparticulate porosity associated with the meso- and macro-structures of the samples.²⁶ Hysteresis was observed persisting to low relative pressures for all of the copolymers, particularly for CP-CMP5 and CP-CMP6, which is consistent with elastic deformations or swelling as a result of gas sorption.³⁸ The apparent BET surface area for these copolymer networks was found not fall into a simple and rational order. For example, we did not observe that the surface area to simply increase or decrease with increasing TBrCz content from CM-CMP1 to CM-CMP7. Among the seven copolymer networks, CP-CMP5 with 60 mol% TBrCz shows the highest BET surface area up to $2241 \text{ m}^2 \text{ g}^{-1}$, which is much higher than that of CP-CMP1 ($1191 \text{ m}^2 \text{ g}^{-1}$) without carbazole unit and CP-CMP7 ($847 \text{ m}^2 \text{ g}^{-1}$) without pyrene unit. This could be partially explained by the different activity of TBrCz and TBrPy in Suzuki coupling reaction, as thus, it is unlikely that the five random copolymers (CP-CMP2–6) were formed by incorporating both comonomers of TBrCz and TBrPy at the same rate, which leads to the complicated series structure of carbazole and pyrene units in the polymer chain and different geometric configuration from those of the alternating copolymers of CP-CMP1 and

CP-CMP7. We need to point out that this result is different from that of most other reported copolymer networks produced from copolymerization using two or three comonomers, where the surface area of the copolymer networks lies “between” both of homocoupling polymers without a second comonomer.²⁶⁻²⁹ We do not at present have a full explanation for this unusual observation, but the repeated experiments demonstrated that all of the copolymer networks are good reproducible in both BET surface area and micropore surface area from batch to batch (Table S1). The copolymer networks showed the standard deviation of BET surface area between 25 (for CP-CMP7) and 64 (for CP-CMP5) with the standard deviation of micropore surface area in the range from 16 to 52. In addition, the shape of nitrogen adsorption / adsorption isotherms is very similar for each sample produced from different batch (Fig. S5–S11). The surface area of 2241 m² g⁻¹ for CP-CMP5 is much higher than that of most reported CMPs, such as poly(aryleneethynylene)-based CMPs (522–1018 m² g⁻¹),²⁶ homocoupled poly(phenylene butadiynylene) CMPs (827–842 m² g⁻¹),³⁹ functionalized CMPs (3–880 m² g⁻¹),⁴⁰ pyrene-based fluorescent CMPs (303–1508 m² g⁻¹),¹⁶ spiro-bipropylendioxythiophene-based CMPs (1334–1631 m² g⁻¹),³³ and comparable to that of carbazole-based CMP (2220 m² g⁻¹),³⁶ although it is lower than that of PAF-1 (5640 m² g⁻¹) produced from tetrakis(4-bromophenyl)methane by Yamamoto polymerization.³⁵ Fig. 1b shows the pore size distribution (PSD) curves for the copolymer networks as calculated using nonlocal density functional theory (NL-DFT). As shown in Fig. 1b, all of the copolymer networks show dominantly micropore size distribution with pore diameter less than 2 nm, while CP-CMP7 without pyrene unit shows the smallest micropore diameter centered around at 0.9 nm, and CP-CMP1–4 show the micropore diameter around at 1.0 nm. However, CP-CMP5 and CP-CMP6 show bigger micropore diameter around at 1.1 nm and with

broad pore size distribution, which is in good agreement with the N_2 adsorption isotherms. These results demonstrated that the ratio of the comonomers (e.g. TBrPy and TBrCz) has a large influence on the pore properties of these copolymers such as surface area and pore size. Therefore, there would be a wealth of opportunity for tuning the surface area and pore size of other type POPs via statistical copolymerization by using other building blocks.

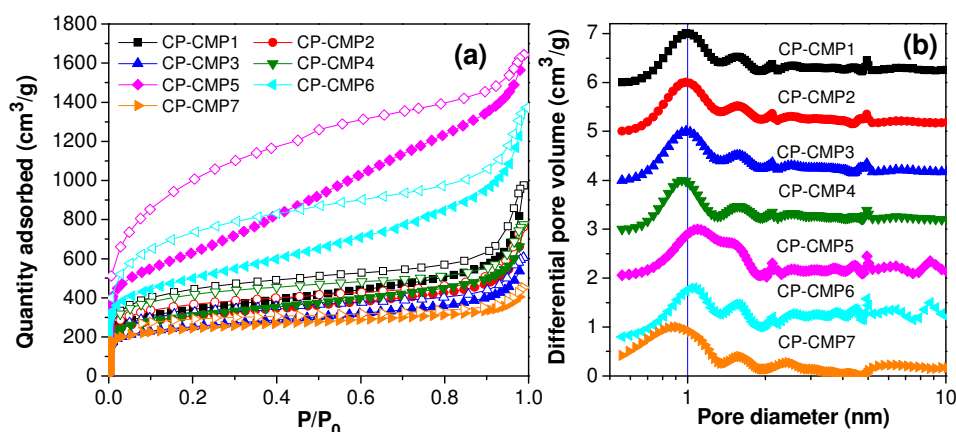


Fig. 1 (a) Nitrogen adsorption (filled symbols) and desorption (open symbols) isotherms for the copolymer networks, (b) Pore size distribution curves calculated from NL-DFT for the copolymer networks.

Table 1 Summary of pore properties for the copolymer networks

Copolymer	BDA [mmol]	TBrPy [mmol]	TBrCz [mmol]	S_{BET}^a [$m^2 g^{-1}$]	S_{Micro}^b [$m^2 g^{-1}$]	V_{Total}^c [$cm^3 g^{-1}$]	V_{Micro}^d [$cm^3 g^{-1}$]
CP-CMP1	2.0	1.0	0	1191	801	0.87	0.39
CP-CMP2	2.0	0.8	0.2	1067	796	0.72	0.38
CP-CMP3	2.0	0.6	0.4	883	632	0.62	0.31
CP-CMP4	2.0	0.5	0.5	1083	754	0.76	0.37
CP-CMP5	2.0	0.4	0.6	2241	1129	2.07	0.80
CP-CMP6	2.0	0.2	0.8	1764	909	1.46	0.47
CP-CMP7	2.0	0	1.0	847	699	0.53	0.34

^a Surface area calculated from N_2 adsorption isotherm in the relative pressure (P/P_0) range from 0.05 to 0.20, ^b Micropore surface area calculated from the N_2 adsorption isotherm using t-plot method based on the Harkins-Jura Equation, ^c Total pore volume at $P/P_0 = 0.90$, ^d The micropore volume derived from the t-plot method.

The high BET specific surface area and the microporous nature of the copolymer networks inspired us to investigate their gas uptake abilities. Fig. 2a shows the hydrogen sorption curves of the seven copolymer networks at 77.3 K up to a pressure of 1.13 bar. CP-CMP5, possessing the highest apparent BET surface area, exhibits the largest H₂ uptake ability of 2.24 wt% at 1.13 bar/77.3 K, while CP-CMP3 shows the lowest H₂ uptake capacity of 0.93 wt%, which could be attributed to its lowest micropore surface area and micropore volume among the resulting copolymer networks (Table 1). In addition, it was found that the H₂ uptake ability of these copolymer networks increases with increasing micropore surface area and micropore volume (Table 1 and Fig. 2), since micropores, not mesopores, mostly contribute to the H₂ adsorption at these pressures and temperatures.³⁹ The hydrogen uptake capacity of 2.24 wt% for CP-CMP5 is higher than that of most reported CMPs under the same conditions, such as the poly(aryleneethynylene) CMPs (1.4 wt% for CMP-0),²⁶ the spiro-bipropylenedioxythiophene-based CMPs (1.72 wt% for SPT-CMP-1),³³ the fluorine-rich CMP (1.14 wt%),⁴⁰ and hexaphenylbenzene-based CMPs (1.50 wt% for HPOP-1),⁴¹ although it is still lower than the carbazole-based CMP with the hydrogen uptake capacity of 2.80 wt% at 1.13 bar/77.3 K.³⁶

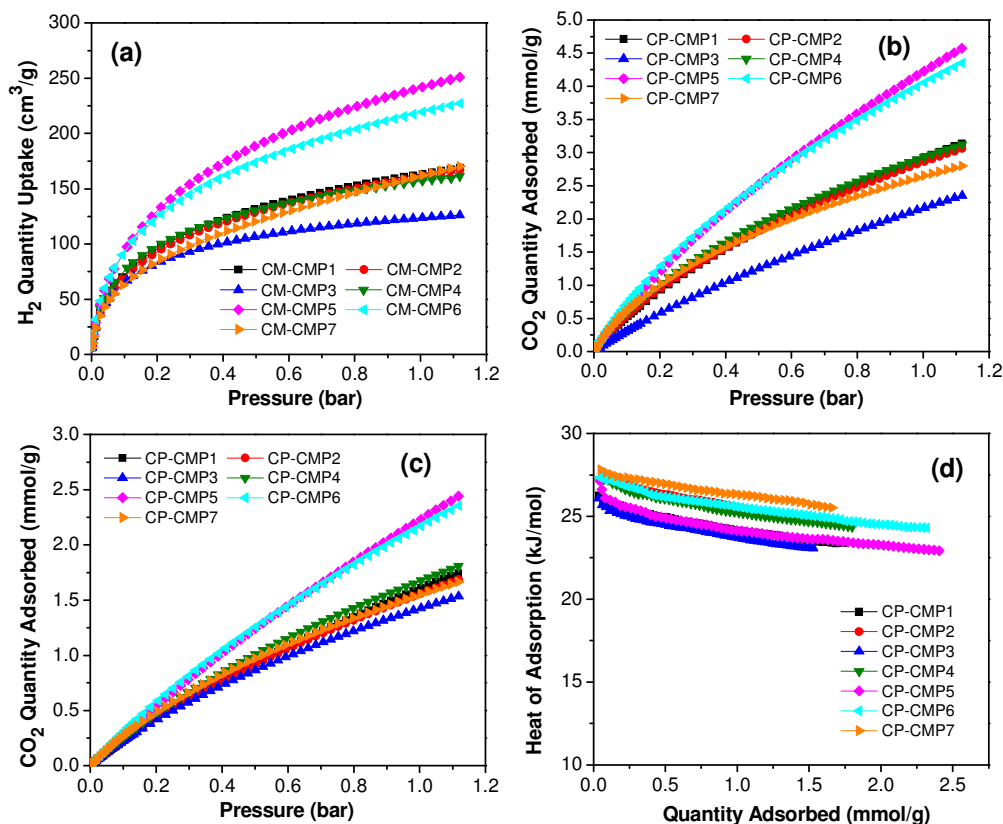


Fig. 2 (a) Volumetric H₂ adsorption isotherms collected at 77.3 K, (b) CO₂ adsorption isotherms at 273 K, (c) CO₂ adsorption isotherms at 298 K, (d) Isothermic heats of adsorption for CO₂ for the copolymers.

The CO₂ uptakes of the copolymer networks were measured up to 1.13 bar at 273 and 298 K, respectively (Fig. 2b & 2c). As expected, the most porous polymer CP-CMP5 shows a high CO₂ uptake ability of 4.57 mmol g⁻¹ at 1.13 bar/273 K, which is much higher than that of CP-CMP1 (3.14 mmol g⁻¹) without carbazole unit and CP-CMP7 (2.80 mmol g⁻¹) without pyrene unit. The high CO₂ uptake ability of CP-CMP5 could be attributed to its high surface area and high nitrogen content. The CO₂ uptake of 4.57 mmol g⁻¹ for CP-CMP5 is much higher than that of most other reported POPs under the same conditions, such as the triazine-based CMPs (1.22–2.62 mmol g⁻¹),⁴² the functionalized CMPs (1.6–1.8 mmol g⁻¹),¹³ the conjugated microporous polytriphenylamine networks (0.5–1.48 mmol g⁻¹),⁴³ the PAFs (2.1–2.4 mmol g⁻¹),⁴⁴ and the carbazole-based HCPs (3.23–3.82 mmol g⁻¹),⁴⁵ and also

comparable to the triazine-based TSP-2 (4.10 mmol g^{-1}),⁴⁶ the carbazolic porous organic frameworks (4.77 mmol g^{-1}),⁴⁷ the benzimidazole-linked polymers (5.45 mmol g^{-1} for BILP-4),⁴⁸ fluorinated covalent triazine-based frameworks (5.53 mmol g^{-1} for FCTF-1-600),⁴⁹ and the imine-linked porous polymer frameworks (6.1 mmol g^{-1} for PPF-1).⁵⁰

To determine the binding affinity between the copolymer networks and CO_2 molecules, the isosteric heat of adsorption (Q_{st}) was calculated from the Clausius–Clapeyron equation using the CO_2 adsorption data collected at 273 K and 298 K. As shown in Fig. 2d, All of the copolymer networks show high isosteric heats of CO_2 adsorption over 26 kJ mol^{-1} at the near zero coverage. CP-CMP7 shows the highest Q_{st} ($27.83 \text{ kJ mol}^{-1}$) at the zero-coverage among the seven copolymer networks, which could be attributed to the smallest micropore size in CP-CMP7 as discussed above, small pore sizes known to increase the heat of adsorption,⁵¹ and its highest nitrogen content, as evidenced by elemental analysis, which enhanced the interactions between the polymer network and CO_2 molecules. However, as the lower surface area and pore volume, CP-CMP7 shows lower CO_2 adsorption (2.80 mmol g^{-1}) than CP-CMP5 (4.57 mmol g^{-1}) at 1.13 bar/273 K. It was found that the Q_{st} values for the copolymer networks can remain nearly constant over a wide range of CO_2 loading, which suggests that a significantly higher CO_2 uptake could probably be achieved by increasing the micropore surface area and micropore volume of the adsorbent.

Table 2 Summary of gas uptakes for the copolymer networks

Copolymer	H ₂ uptake ^a	CO ₂ uptake ^b	CH ₄ uptake ^b	CO ₂ uptake ^c	Selectivity ^d	
	[wt%]	[mmol g ⁻¹]	[mmol g ⁻¹]	[mmol g ⁻¹]	CO ₂ /N ₂	CO ₂ /CH ₄
CP-CMP1	1.51	3.14	1.16	1.75	21.7	3.4
CP-CMP2	1.49	3.06	1.01	1.69	22.1	4.0
CP-CMP3	1.13	2.35	0.93	1.53	25.6	3.9
CP-CMP4	1.44	3.12	1.11	1.81	24.2	4.0
CP-CMP5	2.24	4.57	1.43	2.44	20.5	3.9
CP-CMP6	2.03	4.35	1.37	2.35	23.9	4.2
CP-CMP7	1.42	2.80	0.74	1.66	40.6	6.0

^a Data collected by volumetric H₂ sorption method at 77.3 K and 1.13 bar, ^b Data collected at 273 K and 1.13 bar, ^c Data collected at 298 K and 1.13 bar, ^d Adsorption selectivity based on the Henry's law.

The methane sorption performance of the copolymer networks was also explored (Fig. S12). Among the resulting copolymer networks, CP-CMP5 with the highest surface area exhibits the largest methane uptake ability of 1.43 mmol g⁻¹ at 1.13 bar/273 K (Table 2). This value is comparable to that of the porous benzimidazole-linked polymers (0.87–1.62 mmol g⁻¹),⁴⁸ the porous aromatic frameworks produced by AlCl₃-catalyzed coupling polymerization (0.60–1.04 mmol g⁻¹),⁵² and the carbazolic porous organic frameworks (0.65~1.58 mmol g⁻¹)⁴⁷ under the same conditions. In order to investigate the gas adsorption selectivity of the microporous polymer networks, CO₂, CH₄ and N₂ sorption properties were measured by volumetric methods at the same conditions. The gas adsorption selectivity was estimated using the ratios of the Henry's law constants calculated from the initial slopes of the single-component gas adsorption isotherms at low pressure coverage (< 0.15 bar). The calculated CO₂/CH₄ adsorption selectivity was about 4.0 for most of the copolymer networks (Table 2), which is comparable to that of some reported POPs, such as the carbazole-spacer-carbazole based CMPs with the CO₂/CH₄ selectivity of 4,⁵³ the carbazolic porous organic frameworks (4.4–7.1),⁴⁷ although it is

lower than that of the porous benzimidazole-linked polymers (8–17).⁴⁸ The calculated CO₂/N₂ adsorption selectivity for these copolymer networks varied between 20.5 and 40.6. Among the seven copolymer networks, CP-CMP5 shows the lowest CO₂/N₂ adsorption selectivity (Table 2), although it exhibits the highest surface area and the highest CO₂ uptake ability, which is most likely due to its larger pores as discussed above that are more accessible by N₂ molecules. In addition, CP-CMP7, which has the smallest pore size with highest percentage of micropores among the seven copolymer networks, shows the highest CO₂/N₂ adsorption selectivity of 40.6. Similar result was also observed for other POPs.^{47, 54} Though the CO₂/N₂ adsorption selectivities for these copolymer networks are moderate compared with those of some other reported POPs with the CO₂/N₂ adsorption selectivity higher than 100, such as the porous covalent electron-rich organonitridic frameworks (109 for PECONF-1),⁵⁵ the N₂-phobic nanoporous covalent organic polymers (110 for azo-COP-2),⁵⁶ and the tetraphenylethylene-based HCPs (119 for Network-7),²⁸ most of the copolymer networks show much higher CO₂ adsorption capacity (PECONF-1, 1.86 mmol g⁻¹; azo-COP-2, 2.55 mmol g⁻¹; Network-7, 1.92 mmol g⁻¹) under the same conditions. Ideally, high CO₂ uptake and CO₂/N₂ adsorption selectivity are both required for practical applications. As such, the high CO₂ uptake capacity and the good CO₂/N₂ adsorption selectivity by these copolymer networks make them promising candidates for applications in post-combustion CO₂ capture and sequestration technology.

Conclusion

In conclusion, a series of conjugated microporous copolymer networks was synthesized by Suzuki cross-coupling copolymerization of 1,4-benzene diboronic acid with comonomers of 1,3,6,8-tetrabromopyrene and/or 1,3,6,8-tetrabromocarbazole in a number of ratios. These resulting copolymer networks are stable in common organic

solvents and thermally stable. It was found that the pore properties (e.g. surface area, pore size and pore volume) of these copolymer networks are closely related to the feed ratio of the comonomers of 1,3,6,8-tetrabromopyrene or 1,3,6,8-tetrabromocarbazole. Among the seven resulting copolymer networks, CP-CMP5 with 60 mol% 1,3,6,8-tetrabromocarbazole shows the highest BET specific surface area up to 2241 m² g⁻¹ and a high CO₂ uptake ability of 4.57 mmol g⁻¹ (1.13 bar/273 K) with a H₂ uptake ability of 2.24 wt% (1.13 bar/77.3 K). These results demonstrated that there is a wealth of opportunity for producing microporous organic copolymers with improved surface area and enhanced gas adsorption ability by statistical copolymerization.

Electronic supplementary information (ESI) available: Details of the synthesis for CM-CMP2–CM-CMP7 and the TGA, FT-IR, PXRD, SEM images, and gas adsorption for the copolymer networks. See DOI:XXX/XXX.

Acknowledgments

This work was supported by the National Natural Science Foundation of China (21304055), Research Fund for the Doctoral Program of Higher Education of China (20120202120007), Science and Technology Program of Shaanxi Province (2013KJXX-72), Shaanxi Innovative Team of Key Science and Technology (2013KCT-17), and the Fundamental Research Funds for the Central Universities (GK201501002, GK201101003 & GK201301002).

Notes and references

1. F. Li and L.-S. Fan, *Energy Environ. Sci.*, 2008, **1**, 248-267.
2. F. S. Su, C. Y. Lu, S. C. Kuo and W. T. Zeng, *Energy Fuels*, 2010, **24**, 1441-1448.
3. C. Lu, H. Bai, B. Wu, F. Su and J. F. Hwang, *Energy Fuels*, 2008, **22**, 3050-3056.

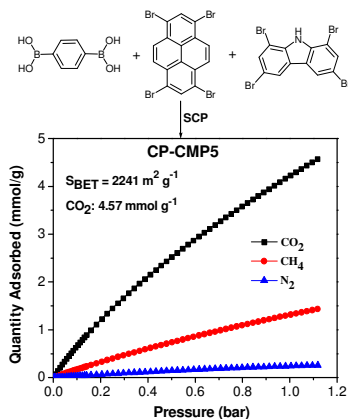
4. K. Sumida, D. L. Rogow, J. A. Mason, T. M. McDonald, E. D. Bloch, Z. R. Herm, T.-H. Bae and J. R. Long, *Chem. Rev.*, 2011, **112**, 724-781.
5. R. Dawson, E. Stockel, J. R. Holst, D. J. Adams and A. I. Cooper, *Energy Environ. Sci.*, 2011, **4**, 4239-4245.
6. N. B. McKeown and P. M. Budd, *Macromolecules*, 2010, **43**, 5163-5176.
7. C. F. Martin, E. Stockel, R. Clowes, D. J. Adams, A. I. Cooper, J. J. Pis, F. Rubiera and C. Pevida, *J. Mater. Chem.*, 2011, **21**, 5475-5483.
8. S. Y. Ding and W. Wang, *Chem. Soc. Rev.*, 2013, **42**, 548-568.
9. Y. Xu, S. Jin, H. Xu, A. Nagai and D. Jiang, *Chem. Soc. Rev.*, 2013, **42**, 8012-8031.
10. D. Yuan, W. Lu, D. Zhao and H. C. Zhou, *Adv. Mater.*, 2011, **23**, 3723-3725.
11. J.-X. Jiang, F. Su, A. Trewin, C. D. Wood, N. L. Campbell, H. Niu, C. Dickinson, A. Y. Ganin, M. J. Rosseinsky, Y. Z. Khimyak and A. I. Cooper, *Angew. Chem. Int. Ed.*, 2007, **46**, 8574-8578.
12. A. I. Cooper, *Adv. Mater.*, 2009, **21**, 1291-1295.
13. R. Dawson, D. J. Adams and A. I. Cooper, *Chem. Sci.*, 2011, **2**, 1173-1177.
14. Y. Kou, Y. Xu, Z. Guo and D. Jiang, *Angew. Chem. Int. Ed.*, 2011, **50**, 8753-8757.
15. L. Chen, Y. Honsho, S. Seki and D. L. Jiang, *J. Am. Chem. Soc.*, 2010, **132**, 6742-6748.
16. J.-X. Jiang, A. Trewin, D. J. Adams and A. I. Cooper, *Chem. Sci.*, 2011, **2**, 1777-1781.
17. Y. Xu, L. Chen, Z. Guo, A. Nagai and D. Jiang, *J. Am. Chem. Soc.*, 2011, **133**, 17622-17625.
18. C. Gu, Y. Chen, Z. Zhang, S. Xue, S. Sun, K. Zhang, C. Zhong, H. Zhang, Y. Pan, Y. Lv, Y. Yang, F. Li, S. Zhang, F. Huang and Y. Ma, *Adv. Mater.*, 2013, **25**, 3443-3448.
19. L. Chen, Y. Yang and D. L. Jiang, *J. Am. Chem. Soc.*, 2010, **132**, 9138-9143.
20. X. Du, Y. Sun, B. Tan, Q. Teng, X. Yao, C. Su and W. Wang, *Chem. Commun.*, 2010, **46**, 970-972.
21. J.-X. Jiang, C. Wang, A. Laybourn, T. Hasell, R. Clowes, Y. Z. Khimyak, J. L. Xiao, S. J. Higgins, D. J. Adams and A. I. Cooper, *Angew. Chem. Int. Ed.*, 2011, **50**, 1072-1075.
22. Z. Xie, C. Wang, K. E. deKrafft and W. Lin, *J. Am. Chem. Soc.*, 2011, **133**, 2056-2059.
23. Y. Xie, T.-T. Wang, X.-H. Liu, K. Zou and W.-Q. Deng, *Nat. Commun.*, 2013, **4**, 1960.

24. V. Guillerm, L. J. Weselinski, M. Alkordi, M. I. H. Mohideen, Y. Belmabkhout, A. J. Cairns and M. Eddaoudi, *Chem. Commun.*, 2014, **50**, 1937-1940.
25. S. Sung and M. P. Suh, *J. Mater. Chem. A*, 2014, **2**, 13245-13249.
26. J.-X. Jiang, F. Su, A. Trewin, C. D. Wood, H. Niu, J. T. A. Jones, Y. Z. Khimyak and A. I. Cooper, *J. Am. Chem. Soc.*, 2008, **130**, 7710-7720.
27. R. Dawson, T. Ratvijitvech, M. Corker, A. Laybourn, Y. Z. Khimyak, A. I. Cooper and D. J. Adams, *Polym. Chem.*, 2012, **3**, 2034-2038.
28. S. Yao, X. Yang, M. Yu, Y. Zhang and J.-X. Jiang, *J. Mater. Chem. A*, 2014, **2**, 8054-8059.
29. C. Pei, T. Ben, Y. Li and S. Qiu, *Chem. Commun.*, 2014, **50**, 6134-6136.
30. H. X. Deng, C. J. Doonan, H. Furukawa, R. B. Ferreira, J. Towne, C. B. Knobler, B. Wang and O. M. Yaghi, *Science*, 2010, **327**, 846-850.
31. G. Venkataramana and S. Sankararaman, *Eur. J. Org. Chem.*, 2005, **2005**, 4162-4166.
32. H. Huang, Q. Fu, B. Pan, S. Zhuang, L. Wang, J. Chen, D. Ma and C. Yang, *Org. Lett.*, 2012, **14**, 4786-4789.
33. J.-X. Jiang, A. Laybourn, R. Clowes, Y. Z. Khimyak, J. Bacsa, S. J. Higgins, D. J. Adams and A. I. Cooper, *Macromolecules*, 2010, **43**, 7577-7582.
34. S. Yuan, B. Dorney, D. White, S. Kirklín, P. Zapol, L. Yu and D.-J. Liu, *Chem. Commun.*, 2010, **46**, 4547-4549.
35. T. Ben, H. Ren, S. Ma, D. Cao, J. Lan, X. Jing, W. Wang, J. Xu, F. Deng, J. M. Simmons, S. Qiu and G. Zhu, *Angew. Chem. Int. Ed.*, 2009, **48**, 9457-9460.
36. Q. Chen, M. Luo, P. Hammershoj, D. Zhou, Y. Han, B. W. Laursen, C. G. Yan and B. H. Han, *J. Am. Chem. Soc.*, 2012, **134**, 6084-6087.
37. K. S. W. Sing, D. H. Everett, R. A. W. Haul, L. Moscou, R. A. Pierotti, J. Rouquerol and T. Siemieniewska, *Pure Appl. Chem.*, 1985, **57**, 603-619.
38. J. Weber, M. Antonietti and A. Thomas, *Macromolecules*, 2008, **41**, 2880-2885.
39. J.-X. Jiang, F. Su, H. J. Niu, C. D. Wood, N. L. Campbell, Y. Z. Khimyak and A. I. Cooper, *Chem. Commun.*, 2008, 486-488.
40. R. Dawson, A. Laybourn, R. Clowes, Y. Z. Khimyak, D. J. Adams and A. I. Cooper, *Macromolecules*, 2009, **42**, 8809-8816.

41. Q. Chen, M. Luo, T. Wang, J.-X. Wang, D. Zhou, Y. Han, C.-S. Zhang, C.-G. Yan and B.-H. Han, *Macromolecules*, 2011, **44**, 5573-5577.
42. S. Ren, R. Dawson, A. Laybourn, J.-X. Jiang, Y. Khimyak, D. J. Adams and A. I. Cooper, *Polym. Chem.*, 2012, **3**, 928-934.
43. Y. Liao, J. Weber and C. F. J. Faul, *Chem. Commun.*, 2014, **50**, 8002-8005.
44. T. Ben, C. Pei, D. Zhang, J. Xu, F. Deng, X. Jing and S. Qiu, *Energy Environ. Sci.*, 2011, **4**, 3991-3999.
45. J.-H. Zhu, Q. Chen, Z.-Y. Sui, L. Pan, J. Yu and B.-H. Han, *J. Mater. Chem. A*, 2014, **2**, 16181-16189.
46. X. Zhu, S. M. Mahurin, S. H. An, C. L. Do-Thanh, C. Tian, Y. Li, L. W. Gill, E. W. Hagaman, Z. Bian, J. H. Zhou, J. Hu, H. Liu and S. Dai, *Chem. Commun.*, 2014, **50**, 7933-7936.
47. X. Zhang, J. Lu and J. Zhang, *Chem. Mater.*, 2014, **26**, 4023-4029.
48. M. G. Rabbani and H. M. El-Kaderi, *Chem. Mater.*, 2012, **24**, 1511-1517.
49. Y. Zhao, K. X. Yao, B. Teng, T. Zhang and Y. Han, *Energy Environ. Sci.*, 2013, **6**, 3684-3692.
50. Y. Zhu, H. Long and W. Zhang, *Chem. Mater.*, 2013, **25**, 1630-1635.
51. J. Germain, J. M. J. Fréchet and F. Svec, *Small*, 2009, **5**, 1098-1111.
52. L. Li, H. Ren, Y. Yuan, G. Yu and G. Zhu, *J. Mater. Chem. A*, 2014, **2**, 11091-11098.
53. S. Qiao, Z. Du and R. Yang, *J. Mater. Chem. A*, 2014, **2**, 1877-1885.
54. R. Dawson, A. I. Cooper and D. J. Adams, *Polym. Int.*, 2013, **62**, 345-352.
55. P. Mohanty, L. D. Kull and K. Landskron, *Nat. Commun.*, 2011, **2**, 401.
56. H. A. Patel, S. H. Je, J. Park, Y. Jung, A. Coskun and C. T. Yavuz, *Chem. – A Eur. J.*, 2014, **20**, 772-780.

Table of Contents

Conjugated microporous copolymer networks show a high specific surface area up to $2241 \text{ m}^2 \text{ g}^{-1}$ and a high CO_2 uptake ability of 4.57 mmol g^{-1} (1.13 bar/273 K) with a H_2 uptake ability of 2.24 wt% (1.13 bar/77.3 K).

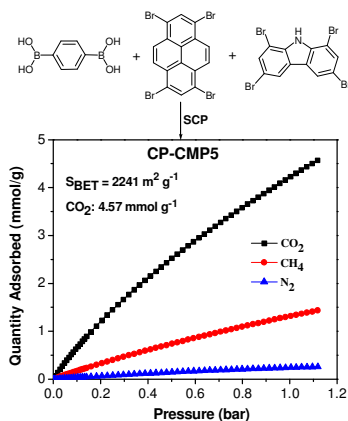


Miao Yu, Xiaoyan Wang, Xiao Yang, Yang Zhao, Jia-Xing Jiang*

Conjugated Microporous Copolymer Networks with Enhanced Gas Adsorption

Graphical Abstract

Conjugated microporous copolymer networks show a high specific surface area up to $2241 \text{ m}^2 \text{ g}^{-1}$ and a high CO_2 uptake ability of 4.57 mmol g^{-1} (1.13 bar/273 K) with a H_2 uptake ability of 2.24 wt% (1.13 bar/77.3 K).



Miao Yu, Xiaoyan Wang, Xiao Yang, Yang Zhao, Jia-Xing Jiang*

Conjugated Microporous Copolymer Networks with Enhanced Gas Adsorption